The Journal of Neuroscience, November 1, 1999, *19*(21):9149–9159

Ca^{2+} Permeation of AMPA Receptors in Cerebellar Neurons Expressing Glu Receptor 2

James R. Brorson, Zehui Zhang, and Wim Vandenberghe

Department of Neurology and Committees on Neurobiology and Cell Physiology, The University of Chicago, Chicago, Illinois 60637

AMPA receptors in cultured cerebellar neurons were characterized by whole-cell electrophysiological studies and single cell PCR-based quantitation of subunit mRNA expression. Purkinje neurons consistently expressed high levels of Glu receptor 2 (GluR2) mRNA and AMPA receptors with low but nonzero Ca^{2+} permeability. Other cerebellar neurons expressed AMPA receptors with a wide range of Ca^{2+} permeability and of fractional GluR2. These properties correlated on a cell-by-cell basis. Their relationship was well fit by a model that assumed stochastic assembly of subunits and GluR2 dominance in controlling divalent cation permeation, suggesting that AMPA receptor properties in individual neurons may be determined primarily by relative levels of subunit transcription. A fraction of receptors, lacking GluR2, can contribute a highly Ca^{2+}-permeable component to AMPA receptor responses, even in cells expressing GluR2.

Key words: excitotoxicity; glutamate; AMPA; transcription; permeability; receptor assembly

An important role for AMPA receptors in Ca^{2+}- mediated glutamate excitotoxicity has been demonstrated in several neuronal systems. AMPA receptor activation can produce Ca^{2+}-dependent excitotoxicity by indirect means, leading to toxic Ca^{2+} entry via voltage-gated Ca^{2+} channels or through Na^+ loading and subsequent reversal of Ca^{2+}–Na^+ exchange. Suggestive evidence has also linked direct permeation of Ca^{2+} ions through the AMPA receptor ion pore to subsequent toxic death in selected types of neurons (Brorson et al., 1994; Turetsky et al., 1994; Carriedo et al., 1996). Because the Ca^{2+} permeability and rectification of AMPA receptors are controlled by the presence or absence of the Glu receptor 2 (GluR2) subunit (Hollmann et al., 1991; Bochet et al., 1994), it is often assumed that toxic Ca^{2+} entry through AMPA receptors occurs only via receptor complexes lacking the GluR2 subunit, and that GluR2 expression by a cell prevents any significant Ca^{2+} entry via AMPA receptors. In fact, Ca^{2+} entry via AMPA receptors has been reported even in some cells known to express GluR2 (Brorson et al., 1992; Geiger et al., 1995), and divalent cation permeability rises substantially in cells expressing GluR2 in low amounts relative to the other AMPA receptor subunits (Geiger et al., 1995; Washburn et al., 1997).

How AMPA receptor stoichiometry is regulated in native neurons is not certain. In cells expressing other subunits as well as GluR2, their association into multimeric receptors, if not selectively controlled, may allow a fraction of AMPA receptors to lack GluR2 subunits, resulting in large Ca^{2+} fluxes originating from a small proportion of highly Ca^{2+} permeable receptors in a "mosaic" of AMPA receptors of differing stoichiometries (Burnashev et al., 1992). Intermediate values of AMPA receptor Ca^{2+} permeability, possibly representing such mosaics of receptors, have been observed in various native cells, such as some neurons of the hippocampus (Lerma et al., 1994; Isa et al., 1996), the retina (Zhang et al., 1995), the brainstem (Otis et al., 1995), and the dorsal spinal cord (Goldstein et al., 1995). Alternatively, it is also possible that even receptors containing GluR2 subunits carry modest Ca^{2+} fluxes of magnitude dependent on the receptor subunit composition. The relative contributions of Ca^{2+} entry via GluR2-containing and GluR2-lacking AMPA receptor channels to whole-cell Ca^{2+} loads have not been fully resolved.

To determine the relationship between GluR2 expression and Ca^{2+} permeability of native AMPA receptors, both properties need to be assayed in the same cells. This is possible using single-cell PCR amplification of AMPA receptor subunits after patch-clamp electrophysiological characterization of AMPA receptor properties (Lambolez et al., 1992). Applying these techniques, we have quantified the expression of AMPA receptor subunit message in individual cerebellar neurons and have found that AMPA receptor Ca^{2+} permeability correlates with fractional GluR2 mRNA expression in a manner consistent with a model based on the stochastic assembly of subunits into receptors, dominance of GluR2 in determining Ca^{2+} permeability, and residual small Ca^{2+} permeability in receptors containing GluR2 subunits.

MATERIALS AND METHODS

Neuronal cultures. Dissociated cultures of cerebellar neurons were prepared from day 17 embryonic Sprague Dawley or Holtzman rats (with the sperm-positive day numbered as day 1) as previously described in detail (Brorson et al., 1992). Procedures followed were in accordance with a protocol approved by the University of Chicago Institutional Animal Care and Use Committee. Trypsin-dissociated neurons were plated on 15 mm round glass coverslips and suspended over a feeding glial layer in a serum-free defined medium (N2.1 with 15 mM HEPES added). Neurons for physiological studies were of age 18–35 d *in vitro* (DIV).

Electrophysiology. Whole-cell patch-clamp measurements of ligand-gated currents were performed with solenoid valve-based fast application

Received Jan. 27, 1999; revised Aug. 3, 1999; accepted Aug. 16, 1999.

This work was supported by the Brain Research Foundation and by National Institutes of Health Award RO1 NS36260 (J.R.B.). W.V. is supported as an Aspirant of the Fund for Scientific Research-Flanders. We thank Patricia Manzolillo for skillful technical assistance in developing these techniques, Dr. Yael Stern-Bach, Dr. Todd Verdoorn, Dr. Stephen Heinemann, and Dr. Peter Seeburg for providing AMPA subunit cDNA clones, and Dr. Doris Patneau for helpful comments.

Correspondence should be addressed to Dr. James R. Brorson, Department of Neurology, MC2030, The University of Chicago, 5841 South Maryland Avenue, Chicago, IL 60637. E-mail: jbrorson@neurology.bsd.uchicago.edu.

Table 1. Oligonucleotide primer sequences and preferred PCR conditions

PCR target	Primer	Sequence	T_m (°C)	T_a (°C)
All AMPA subunits	up	5′-CCTTTGGCCTATGAGATCTGGATGTG-3′	78	49
	lo	5′-TCGTACCACCATTTGTTTTTCA-3	60	
GluR1	R1	5′-AGGGACGAGACCAGACAACCAG-3′	70	65
GluR2	R2	5′-ATGGAAGAGAAACACAAAGTAG-3′	60	60
GluR3	C	5′-AGACAACAATGAAGAACCTCGT-3′	62	60
GluR4	R4	5′-GAAGGACCCAGTGACCAGCC-3′	66	65

The estimated melting temperature (T_m) and empirically determined best annealing temperature (T_a) for each PCR reaction are also indicated.

of agonists via a theta tube applicator, as previously described (Brorson et al., 1995). Borosilicate glass pipettes were of resistance 1.7–3 MΩ. Whole-cell resistances were at least 150 MΩ, and access resistances were <10 MΩ. Intracellular solutions for whole-cell recordings contained (in mM): CsF 120, $MgCl_2$ 3, HEPES 10, and EGTA 5, pH to 7.15 with CsOH. Ag-AgCl electrodes served as pipette electrodes and as the ground electrode. The latter was placed in a well containing intracellular solution, which was connected to the extracellular bath via a 3 M KCl-agar bridge. The usual extracellular saline buffer contained (in mM): NaCl 145, KCl 3, $CaCl_2$ 2, $MgCl_2$ 1, HEPES 10, and glucose 10, pH to 7.40 with NaOH. Liquid junction potentials between the pipette solution and this solution, nulled at the start of each recording, measured 0.5–1.5 mV. Current–voltage recordings were not corrected for junction potentials. All experiments were performed at room temperature.

NMDA applications were performed in saline buffer in which Mg^{2+} was omitted and glycine (10 μM) added. Ca^{2+} permeability of AMPA receptors was measured by repeated agonist applications in Na^+-free solutions containing (in mM): $CaCl_2$ 2 or 10, *N*-methyl-D-glucamine (NMG) 145 or 133, $MgCl_2$ 1, CsCl 3, HEPES 10, and glucose 10, with pH adjustment to 7.4 using HCl. Additional recordings used a sucrose-based Ca^{2+} solution containing (in mM): $CaCl_2$ 12.8, $Ca(OH)_2$ 2.2, sucrose 240, HEPES 10, and glucose 10, pH 7.4. To these solutions were added (in μM): tetrodotoxin 0.5, MK-801 (dizocilpine) 1, and Cd^{2+} 100, serving to block synaptic activity, NMDA receptor channels, and voltage-gated Ca^{2+}channels. *I–V* curves were generated from a holding potential of −80 mV and at test potentials varying from −100 mV to +40 mV by 10 mV intervals, with rapid agonist application 300–500 msec after voltage steps. Leak current measured before agonist application was subtracted from peak agonist-evoked current at each potential. Reversal potentials were determined from linear regression of *I–V* data, and relative permeability ratios ($P_{Ca^{2+}}/P_{Cs^+}$) were calculated according to the extended Goldman–Hodgkin–Katz constant field equation (Jan and Jan, 1976; Mayer and Westbrook, 1987; Otis et al., 1995) using estimated ion activities. The permeability of Mg^{2+} relative to that of Ca^{2+} was estimated at 0.8 (Iino et al., 1990). Ion activity coefficients in each solution were estimated from the Debye–Hückel equation based on calculated ionic strengths and estimated effective ionic radii (Dean, 1992). For the 10 mM Ca^{2+}, 145 mM NMG external solution, calculated ionic activity coefficients were for Ca^{2+}, 0.348; for Mg^{2+}, 0.398; for Cs^+, 0.700; and for NMG, 0.782. For the 15 mM Ca^{2+}, sucrose-based external solution, the coefficient for Ca^{2+} was 0.496. Coefficients in the CsF intracellular solution were for Mg^{2+}, 0.416; and for Cs^+, 0.718. AMPA receptors were assumed to be impermeable to anions.

Single-cell PCR. For single-cell PCR, patch-clamp pipettes were silanized, soaked in diethylpyrocarbonate (DEPC)-containing water, and autoclaved before use. The intracellular and extracellular solutions were treated with 0.1% DEPC and autoclaved. All surfaces were wiped in 70% ethanol. Gloves were worn during patch clamping. The RNase-free intracellular solution (4 μl) was back-filled into the pipette after tip filling. After electrophysiological recordings, cell contents were gently aspirated into the pipette. Nuclear material was avoided but sometimes adhered to the pipette tip. The presence of intronic sequences between primer sites prevented contributions of genomic DNA to the PCR product bands, which were of the sizes predicted based on cDNA sequences. The pipette contents were expelled into the reverse transcriptase mix containing 5× first-strand buffer (2.5 μl), dithiothreitol (1 μl), dNTPs (4 μl of a 2.5 mM stock), random hexamers (Pharmacia, Piscataway, NJ; 1 μl of a 2.5 μg/μl stock), RNase inhibitor (RNasin; Promega, Madison, WI; 1 μl or 20 U), and reverse transcriptase (Superscript II; Life Technologies, Gaithersburg, MD; 100 U), to a total volume of 13.5 μl. This reverse transcriptase mixture was incubated at 42°C for 45 min and then at 99°C for 5 min and stored at −20°C until PCR was done.

PCR conditions were similar to those described by Lambolez et al. (1992). Upstream and downstream primers recognized all AMPA receptor subunit sequences (Table 1, up, lo). The entire reverse transcription reaction product was added to a PCR mixture containing standard buffer components (PCR buffer II; Perkin-Elmer, Norwalk, CT), 10 pmol of each primer, 0.05 mM dNTPs (Pharmacia), 2.5 U *Taq* polymerase (Perkin-Elmer), and 1.125 mM $MgCl_2$ (in addition to $MgCl_2$ from the reverse transcription mixture) to a final volume of 100 μl. This mixture, in a thin-walled reaction tube, was covered with oil, placed in the thermal cycler, and denatured at 94°C for 5 min. PCR followed with five ramp cycles of 94°C for 30 sec, 45°C for 30 sec, ramp to 72°C over 1 min 10 sec, and 72°C for 1 min and then 35 cycles to an annealing temperature of 49°C (94°C for 30 sec, 49°C for 30 sec, and 72°C for 1 min). Extension was concluded at 72°C for 10 min. Product (10 μl) was visualized on a 1.0% agarose gel stained with ethidium bromide. Negative controls, from pipettes forming a cell-attached seal without breaking into whole-cell configuration ($n = 16$), and from aspiration of extracellular saline into the pipette for 20 sec ($n = 18$), never produced a visible PCR band. Products of successful reactions were divided in two: most was purified by ethanol precipitation and stored at 4°C until restriction digestion reactions. Ten microliters of PCR product were excised from a low-melting point agarose gel, and the spin column was purified for use in second round, subunit-specific PCR reactions. These were performed in a PCR mixture similar to that given above with 1.5 mM Mg^{2+}, using lo as the downstream primer, and upstream primers and annealing temperatures (T_a) as given in Table 1 for 30 cycles (94°C for 30 sec, T_a for 30 sec, and 72°C for 45 sec), followed by 72°C for 10 min. For subunits present at <0.02 of total product, second-round PCR generally failed to give any product, and splice variant analysis was omitted.

Most of the degenerate first-round PCR product was subjected to restriction enzyme digestion by the four enzymes specific for the AMPA receptor subunits (Table 2), with separation of the products on a non-denaturing polyacrylamide gel. Using the high sensitivity of a double-stranded DNA fluorescent stain (SYBR Green-I; Molecular Probes, Eugene, OR) followed by digital fluorimetric scanning (Storm FluorImager; Molecular Dynamics, Sunnyvale, CA) of the gel allowed detection of fragments in amounts as small as 0.1 ng. Digital images were analyzed by line scan of a central portion of each lane, followed by peak finding and integration (ImageQuant version 1.1, Molecular Dynamics). In analyzing the subunit composition of the degenerate PCR product, the four subunit-specific enzymes were applied simultaneously, analyzing the fractions attributable to each of the subunits from a single lane of the gel. Portions of the PCR product remaining uncut after restriction digestion generally were <0.05 of total; if uncut portions exceeded 0.10 of total, the cell was excluded from analysis. Results from 3 of 56 cerebellar neurons were excluded because of incomplete digestion of PCR products. Activity of restriction enzymes was confirmed on control DNA fragments with each run. Separation of the upper fragments of GluR3 and GluR4 was not complete. To correct for this, the total integrated density of the two overlapping bands was divided proportionately to the relative densities of the lower bands for GluR3 and GluR4 (corrected for length differences), to apportion the overlapping signals to the appropriate subunits. All other digestion fragments were well resolved.

The second-round subunit-specific PCR products, containing both splice variants of the given subunit, were subjected to restriction digestion using the enzymes *Bfa*I to specifically cut GluR1 *flip* splice variants and *Mse*I (for GluR1) or *Hpa*I (for GluR2–4) to specifically cut *flop* splice variants (Table 2). The products were separated on a polyacryl-

Table 2. Restriction enzymes specific for AMPA receptor subunits produced by the PCR products of degenerate primers up and lo and enzymes differentially cutting the *flip* and *flop* splice variants of subunit-specific PCR products

Enzyme	GluR1 (up/lo: 749 bp) (R1/lo: 634 bp)	GluR2 (up/lo: 749 bp) (R2/lo: 634 bp)	GluR3 (up/lo: 755 bp) (C/lo: 651 bp)	GluR4 (up/lo: 749 bp) (R4/lo: 626 bp)
*Bgl*I	+ 448/301	−	−	−
*Bsp*1286I	−	+ 481/268	−	−
*Eco*47III	−	−	+ 401/354	−
*Eco*RI	−	−	−	+ 412/337
*Bfa*I	*flip*: + 570/64 *flop*: −	−	−[a]	+[a] 367/259
*Mse*I	*flip*: − *flop*: + 579/55	*flip*: + 585/49 *flop*: ++ 516/69/49	*flip*: + 586/65 *flop*: +++ 518/65/56/12	*flip*: ++ 503/83/40 *flop*: +++ 516/56/40/14
*Hpa*I	−	*flip*: − *flop*: + 567/67	*flip*: − *flop*: + 584/67	*flip*: − *flop*: + 558/68

Digestion of the PCR product and size of double-stranded DNA fragments produced, in base pairs, are shown.
[a] *Bfa*I also cuts the up and lo PCR products of GluR3 and GluR4 upstream from the nested specific primers.

amide gel and again detected by digital fluorimetric scanning (see Fig. 3*B*). Quantitation of the digested band (corrected for the length difference) compared with the undigested band gave the fractional content for the given subunit of the *flip* or *flop* splice variant. The specificity of the second-round PCR reactions for the target subunits was verified by complete digestion with the subunit-specific restriction enzymes.

To screen for the possibility of incomplete editing of GluR2 message in the cerebellar neurons, specific GluR2 second-round PCR product was also subjected to digestion by *Tse*I, which cleaves the unedited version of the Q/R site but not the edited version of the Q/R site of GluR2. *Tse*I also cuts at a second site in the GluR2 PCR fragment, so that the edited version of the GluR2 PCR product is digested into two fragments, and the unedited version is digested into three fragments. The restriction-digested PCR product was run on a polyacrylamide gel with *Tse*I-digested PCR products of pure edited and unedited sequences as controls, which exhibited clearly distinct patterns of two and three bands, respectively.

Fluorescence imaging and immunocytochemistry. Fluorimetric digital imaging of intracellular $[Ca^{2+}]$ ($[Ca^{2+}]_i$) was performed as described (Brorson et al., 1995) in neurons loaded with 5 μM fura-2 AM (Molecular Probes). Experiments were at room temperature (23°C) in the standard saline buffer. A field of neurons from the central region of a coverslip was selected, and neurons were identified by typical morphology. The average fluorescence at 340 and 380nm illumination was recorded digitally from areas delineated over the soma of each neuron at 2 Hz for the duration of each experiment, and ratios of average emission intensities were converted to approximate $[Ca^{2+}]_i$ by values from a cell-free calibration. After Ca^{2+} imaging experiments, cells were fixed and permeabilized for immunocytochemistry. Immunostaining for calbindin D-28k used a monoclonal antibody (Sigma, St. Louis, MO) and fluorescein- or biotin-tagged secondary antibodies as previously described (Brorson et al., 1995).

Data analysis. Nonlinear regression fitting of reversal potential and fractional GluR2 expression data to predicted equations (see Appendix) were performed using SigmaPlot (SPSS, Inc., Chicago, IL). Significance testing of comparisons of individual parameters between Purkinje cells and non-Purkinje cells, which were of unequal variances, used the Mann–Whitney rank sum test in SigmaStat (SPSS).

Materials. Cloned cDNA for each of the AMPA receptor subunits in both major splice variant forms was kindly provided by Dr. Stephen Heinemann (The Salk Institute, San Diego, CA) and by Dr. Peter Seeburg (University of Heidelberg, Heidelberg, Germany). AMPA and MK-801 were purchased from Research Biochemicals International (Natick, MA). Tetrodotoxin and fura-2 AM were purchased from Molecular Probes. Restriction enzymes were purchased from New England Biolabs (Beverly, MA). Other reagents and chemicals came from Sigma.

RESULTS

Identification of Purkinje cells among cultured cerebellar neurons

The Purkinje cells in primary cultures of cerebellar neurons develop a characteristic morphology and size, with a large round soma giving off one or two primary neurites (Brorson et al., 1992). Their identification can be confirmed by specific staining for the Ca^{2+}-binding protein calbindin D-28k (Fig. 1). Purkinje cells have been found to transiently express functional NMDA receptors during the first weeks of development, but they lack NMDA responses in their mature state (Audinat et al., 1990). This physiological characteristic distinguishes them from other cerebellar neurons and, indeed, from most neurons in the brain. We previously showed that in mature (>17 DIV cultures) cultures, *a priori* identification of the Purkinje cells by morphology reliably predicted the lack of NMDA responsiveness (Brorson et al., 1995). In the present studies, whole-cell responses to kainate, AMPA, and NMDA were recorded in 78 cerebellar neurons. Among neurons identified morphologically as Purkinje cells, significant NMDA-evoked currents (>5% of kainate-evoked cur-

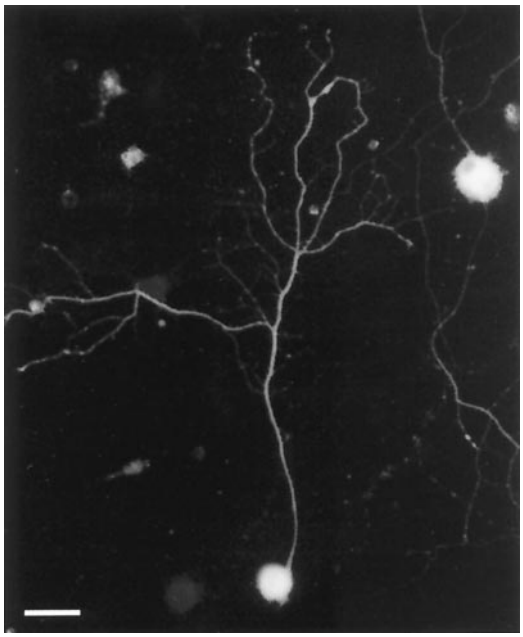

Figure 1. Identification of cultured Purkinje neurons. Cultured cerebellar Purkinje neurons (20 d *in vitro*) were immunostained with monoclonal antibody to calbindin D-28k (Sigma), 1:20,000, and fluoroscein-tagged secondary antibody. Calbindin D-28k-positive Purkinje cells were characterized by a large round soma and one or two long branching primary neurites. Scale bar, 50 μm.

rents) were lacking in 36 of 37 cells, consistent with the morphological identification, whereas 38 of 41 cells identified *a priori* by morphology as non-Purkinje cells (a mixture of cerebellar cortical neurons) exhibited NMDA-evoked responses. Thus these measurements confirmed the general reliability of the morphological identification of the cultured cerebellar neurons, which was used in the studies of the Ca^{2+} permeability of AMPA receptors.

Electrophysiological studies of Ca^{2+} permeability of AMPA receptors in cerebellar neurons

Previous studies have shown that Purkinje cells strongly express GluR2 mRNA (Lambolez et al., 1992; Tempia et al., 1996), suggesting that they would express AMPA receptors with low permeability to Ca^{2+}. To determine Ca^{2+} permeability of expressed AMPA receptors in cultured Purkinje neurons, reversal potentials of the *I–V* relationships of responses to 100 μM kainate were determined in whole-cell voltage-clamp experiments. The kainate-evoked responses in these neurons have been shown to be mediated by AMPA receptors rather than the rapidly desensitizing high-affinity kainate receptors, because they are activated by kainate only at high micromolar concentrations, and they are strongly modulated by cyclothiazide but not concanavalin A (Brorson et al., 1995). To maximize sensitivity to the permeability of Ca^{2+}, *I–V* relationships were measured in the absence of external Na^+, replaced by equimolar NMG, with concentrations of 2 or 10 mM Ca^{2+} externally. To block NMDA channels and voltage-gated Na^+, Ca^{2+}, or K^+ channels, which might interfere with voltage space clamp, 1 μM MK-801, 0.5 μM tetrodotoxin, and 100 μM Cd^{2+} were included, and external K^+ was fully replaced with 3 mM Cs^+. External Cs^+ also contributed to inward AMPA receptor currents, leading to a straightening of the *I–V* curves and to a narrowing of the range of the measured reversal potentials. Under these conditions, kainate evoked small inward currents at the initial holding potential of −80 mV, shifting to larger outward currents at depolarized potentials in all cells studied (Fig. 2). In each cell, *I–V* relationships were measured at external Ca^{2+} of 2 and 10 mM, and the shift in reversal potential with increased Ca^{2+} was observed.

Although positive shifts in reversal potential consistently occurred with increased external Ca^{2+}, there was a clear contrast between the cells identified *a priori* as Purkinje cells and those identified as non-Purkinje cells. In the Purkinje cells, the reversal potential in 2 or 10 mM Ca^{2+} was low, usually below −60 mV, and the shift with increase in Ca^{2+} was always quite small. In contrast, in non-Purkinje cells, there was a wide range in the reversal potential in 10 mM Ca^{2+} from −62 to −26 mV and a corresponding larger range in the shift of the reversal potential with Ca^{2+}. Thus a low but nonzero Ca^{2+} permeability in AMPA receptors of Purkinje cells was confirmed, whereas a wide range of Ca^{2+} permeabilities was indicated for AMPA receptors of other cerebellar cortical neurons.

The reversal potential for a channel can be related to the relative permeabilities of the major ions by the extended Goldman–Hodgkin–Katz (GHK) constant field equation (Hodgkin and Katz, 1949; Jan and Jan, 1976; Mayer and Westbrook, 1987). Although a negligible permeability of AMPA receptors to NMG was previously assumed (Iino et al., 1990), more recent evidence has suggested a small but nonzero permeability via recombinant AMPA receptors even for this bulky organic ion (Burnashev et al., 1996). In the cerebellar neurons, reversal potential measurements in low- and high-concentration NMG solutions were consistent with a permeability of AMPA receptors for NMG of

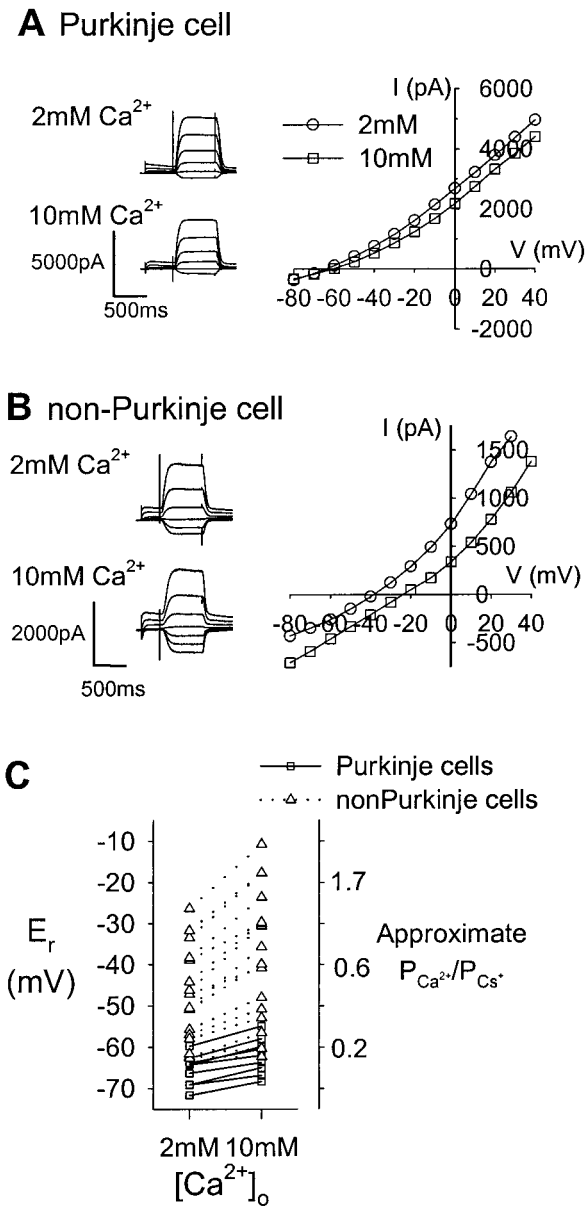

Figure 2. Ca^{2+} conductance of AMPA receptors in cerebellar neurons. Whole-cell currents evoked by application of 100 μM kainate in 2 mM Ca^{2+} and 10 mM Ca^{2+} Na^+-free solutions, at holding potentials ranging from −80 mV to + 40 mV, and resulting leak-subtracted *I–V* relationships in a cultured Purkinje cell with an very low shift in reversal potential (*A*) and in a non-Purkinje cell with a large shift (*B*) are shown. *C*, Summary of reversal potentials of kainate-induced currents in 2 and 10 mM Ca^{2+} for all neurons, with approximate values for $P_{Ca^{2+}}/P_{Cs^+}$, as calculated from the reversal potentials in 10 mM Ca^{2+} using the extended GHK constant field equation. Purkinje cells consistently had low reversal potentials and Ca^{2+} permeabilities but still exhibited small positive shifts of reversal potential with increases in Ca^{2+}. Mean ± SD of reversal potentials in 10 mM Ca^{2+} was −62 ± 4 mV for Purkinje cells and −38 ± 16 mV for non-Purkinje cells ($p < 0.0001$).

~0.14 times that for Ca^{2+} (data not shown). Using this value, and using calculated ion activities for Ca^{2+}, Mg^{2+}, and Cs^{2+}, the permeability of Ca^{2+} relative to that of Cs^+ ($P_{Ca^{2+}}/P_{Cs^+}$) was estimated from the measured reversal potential in 10 mM external Ca^{2+} (Fig. 2*C*). The $P_{Ca^{2+}}/P_{Cs^+}$ in Purkinje cells was 0.22 ± 0.05 (mean ± SD; $n = 9$), contrasting with larger, more widely ranging values for the other cerebellar neurons (0.94 ± 0.72; $n = 16$).

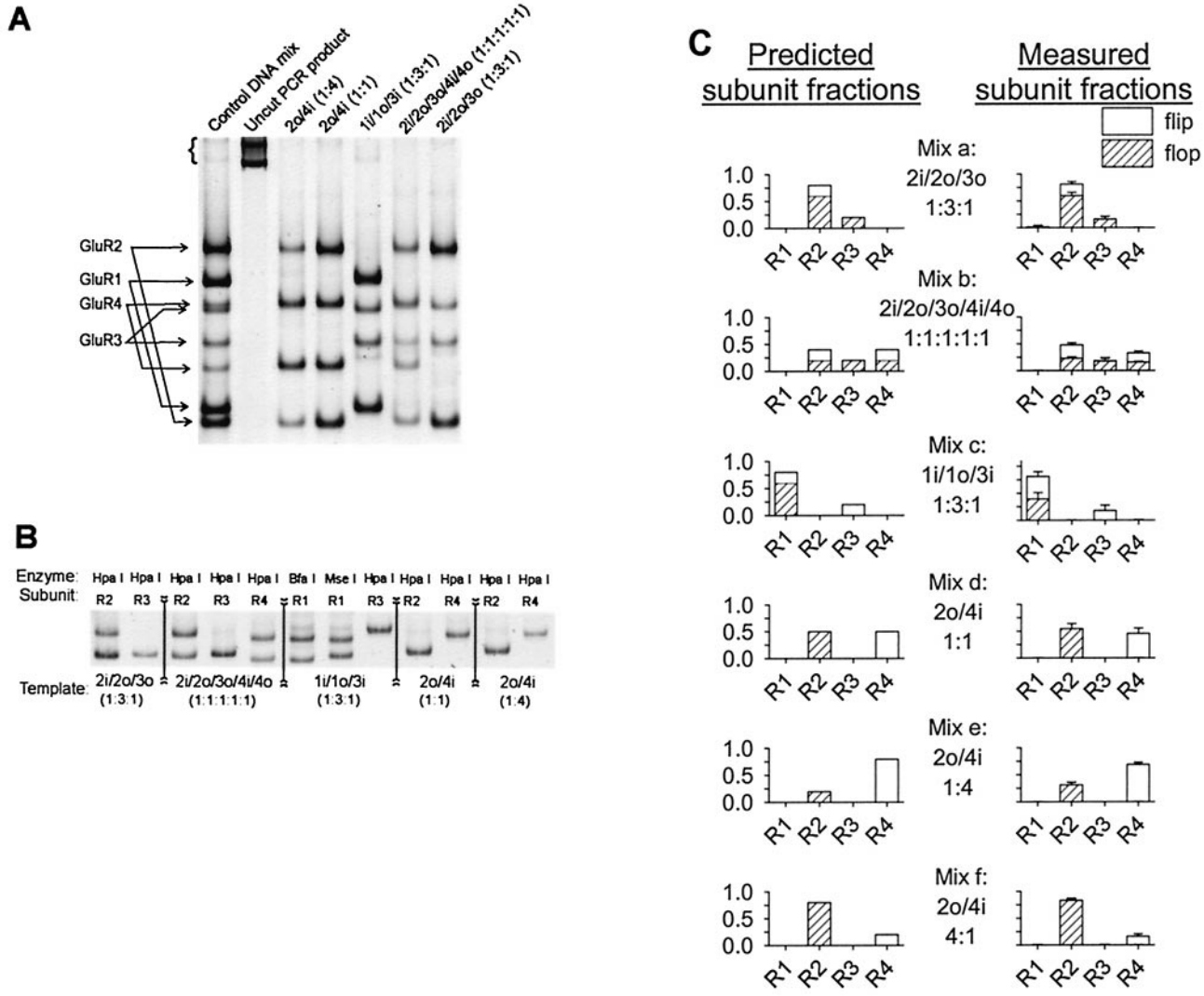

Figure 3. PCR-based assays of subunit composition. Identification of subunit composition of control mixtures of AMPA receptor cRNAs by restriction enzyme digestion and digital fluorimetric detection of DNA bands on a polyacrylamide gel. Control mixtures each contained ~1.2 million total copies of RNA. Their composition is designated by shorthand representation of AMPA subunits (*1i* for GluR1 *flip*, *2o* for GluR2 *flop*, and so forth). *A*, Results of AMPA subunit analysis by digestion with all four subunit-specific enzymes simultaneously applied to degenerate PCR product. Digestion product from a mixture of all four subunits, to localize digested bands, was loaded in the *first lane*; undigested PCR product was loaded in the *second lane* (*bracket*); and product from five control RNA mixtures was loaded in the *third* through *eighth lanes* as indicated. Occasional faint PCR artifacts (*fifth lane*) amounted to <5% of total PCR product. *B*, Restriction enzyme analysis of fractional splice variant composition of AMPA receptor subunits expressed in control mixtures. Product of a second round of PCR using primers specific for the subunit indicated above each lane was subjected to restriction digestion by the indicated enzyme. The template RNA mixture is indicated below each section of the digitally imaged gel. *C*, Quantitation of fractional subunit and splice variant content of control RNA mixtures after reverse transcription PCR. Predicted subunit compositions are depicted at *left*, and the results of repeated assays starting from the same control RNA mixture are plotted at *right* (mean ± SD; $n = 5$).

These values are somewhat greater than those in some previous reports for GluR2-expressing cells (Jonas et al., 1994; Lerma et al., 1994; Geiger et al., 1995). To obtain a more direct measurement of relative Ca^{2+} permeability, eliminating any contribution of NMG, additional kainate-evoked *I–V* curves were elicited from Purkinje neurons in a sucrose-based 15 mM Ca^{2+} solution. In this solution, reversal potentials were -88 ± 2 mV, resulting in $P_{Ca^{2+}}/P_{Cs^+}$ values of 0.10 ± 0.01 ($n = 5$), suggesting a discrepancy between estimates of $P_{Ca^{2+}}/P_{Cs^+}$ in the different solutions.

If AMPA receptors in a given cell constitute a mosaic of receptors of different subunit stoichiometries and differing in their Ca^{2+} permeability and rectification (Burnashev et al., 1992; Washburn et al., 1997), the net whole-cell current at each potential is the sum of currents carried by channels of varying structure. All of the assumptions of the GHK theory, such as uniformity of membrane conductance and ionic independence (Hodgkin and Katz, 1949), may not hold, possibly contributing to differences in calculated values of $P_{Ca^{2+}}/P_{Cs^+}$ under different ionic conditions. As recognized previously by Goldstein et al. (1995), net *I–V* reversal potentials approximate the linear combination of contributions from heterogeneous individual receptors in a cell (see Appendix), and the reversal potential can therefore be used to characterize average cellular Ca^{2+} permeation properties without assumptions about the properties of the ion pore for comparison to receptor subunit expression. For this reason, subsequent analysis used the net reversal potential in 10 mM Ca^{2+}, rather than the estimated $P_{Ca^{2+}}/P_{Cs^+}$, to characterize the Ca^{2+} permeability of AMPA receptors for each cell.

Single-cell PCR

We performed single-cell PCR following a method modified from that of Lambolez et al. (1992). Unlike previous approaches, in these assays fractional AMPA receptor subunit expression was analyzed after a single round of PCR, reducing the potential for nonlinearities resulting from exponential PCR amplification. The four subunit-specific restriction enzymes were applied simultaneously to the PCR product, with separation of products by polyacrylamide gel electrophoresis (Fig. 3*A*). Splice variant composition for each subunit was assessed by a second round of PCR with primers specifically amplifying a single subunit, followed by restriction digestion specific for one of the splice variant forms (Fig. 3*B*). Control mixtures of cRNA transcribed from cDNA clones of the AMPA receptor subunits were designed to span the set of two splice variant isoforms of each of the four subunits and to include combinations of multiple (up to five) RNA species, simulating the natural situation in many neurons. Samples of these cRNA mixtures were subjected to reverse transcription and PCR in dilutions of ~1.2 million copies per PCR reaction, and products were analyzed for subunit and splice variant composition (Fig. 3*C*). Qualitative aspects of subunit and splice variant composition were reproduced with high reliability. Detected quantitative proportions of subunits were similar to those of the original cRNA mixtures, and signals from subunits omitted in the control mixtures were consistently absent (quantified at <0.01 of total).

Because single neurons are expected to have small copy numbers of mRNA for each AMPA subunit (Sucher and Deitcher, 1995), the performance of this assay was tested using additional control mixtures containing ~150 total cRNA molecules (Fig. 4). PCR reactions subjected to 34, 36, 38, and 40 cycles were analyzed separately. The logarithm of the average total DNA signal increased linearly with cycle number, suggesting that over this range the PCR remained exponential. The measured amplification efficiency was ~73% relative to complete doubling of product with each cycle, presumably reduced from the initial efficiency. The fractional representations of individual subunits reflected those predicted from the initial control mixtures and did not systematically change over these cycles, so that even when starting from very low copy numbers, the various subunits were amplified in parallel, preserving the approximate initial proportions. Some inaccuracies in reproducing the predicted subunit compositions might have arisen from errors in initial quantitation of the component cRNAs, but systematic errors of this sort appeared to be modest. SDs in detected subunit fractions, indicating the size of random experimental errors, ranged from 0.01 to 0.10. Thus these two sets of controls confirmed the quantitative reliability of this assay for determining relative proportions of the AMPA subunits from small numbers of RNA molecules.

Characterization of AMPA receptor subunit expression patterns in cerebellar neurons

Single-cell PCR amplification of AMPA receptor subunit expression was successful in 28 of 56 attempts in cerebellar neurons after morphological identification and whole-cell patch-clamp studies. The AMPA receptor subunit expression patterns showed qualitative differences between the Purkinje cells and the non-Purkinje cells (Fig. 5). Purkinje cells consistently expressed high fractions of GluR2, approximately one-half or more of total AMPA subunit mRNA expression, (mean ± SD fractional GluR2, 0.59 ± 0.14) with lesser amounts of GluR1 or GluR3 subunits and little or no GluR4 (<0.02 of total). Most of the total

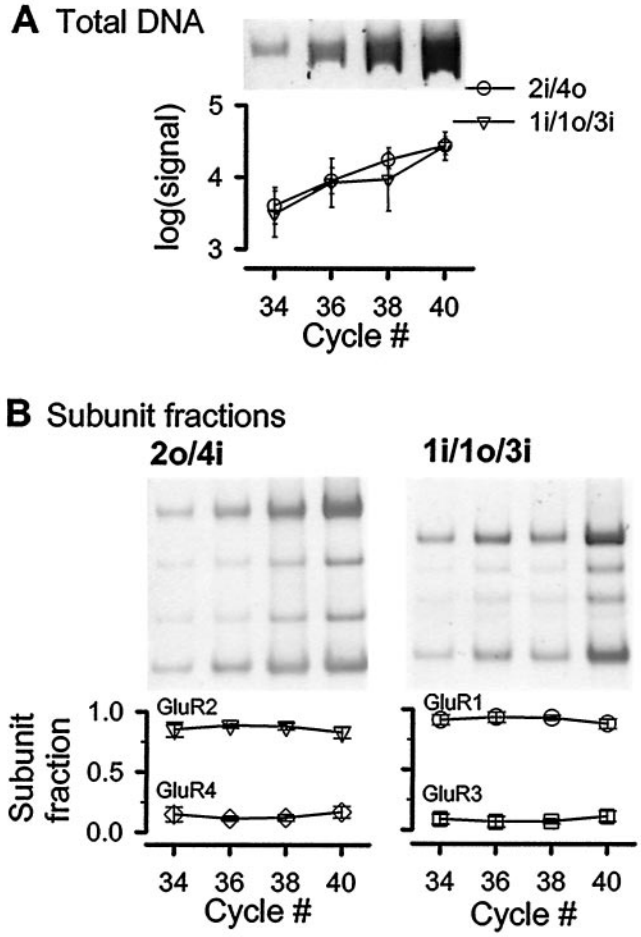

Figure 4. Assay of relative subunit composition from low RNA copy numbers. Additional control mixtures of cRNA were prepared at dilutions producing ~150 total RNA molecules in each sample and were subjected to reverse transcription PCR. PCR samples amplified with 34, 36, 38, and 40 cycles were divided for analysis of total DNA signal (10 μl) and for restriction digestion to determine subunit fractions (90 μl). In total, 36 of 44 PCR reactions were successful in producing visible product. *A*, *Top*, Representative polyacrylamide gel image; *bottom*, logarithm of digital fluorimetric signal of undigested bands versus cycle number (n = 3–5 separate experiments for each point, mean ± SD). Fluorimetric signals corresponded to ~2–3 ng of DNA/1000 U. *B*, *Top*, Representative gel images; *bottom*, subunit fractions calculated from restriction enzyme-digested products versus cycle number from mixtures *2o*/*4i* (1:4) and *1i*/*1o*/*3i* (1:3:1).

subunit expression was in the *flop* isoform, but in two cells, the GluR3 expression was entirely in the *flip* form. This quantitative profile of AMPA subunit expression in cerebellar Purkinje cells is in general agreement with the qualitative results reported in previous studies (Lambolez et al., 1992; Tempia et al., 1996). In contrast to the results in Purkinje cells, the expression pattern varied widely among non-Purkinje cells, reflecting the heterogeneous makeup of this group. The fractional GluR2 content ranged from minimal detectable amounts (Fig. 5*B*,*C*) up to 0.91 (mean ± SD, 0.26 ± 0.25). Some cells expressed measurable amounts of all four subunits, whereas one cell expressed predominantly GluR1 and little of other subunits. The majority of the subunit expression also was of the *flop* isoform in non-Purkinje cells. The average fractional expression of each subunit and of *flip* isoforms, for Purkinje cells and non-Purkinje cells, is shown in Figure 5*D*.

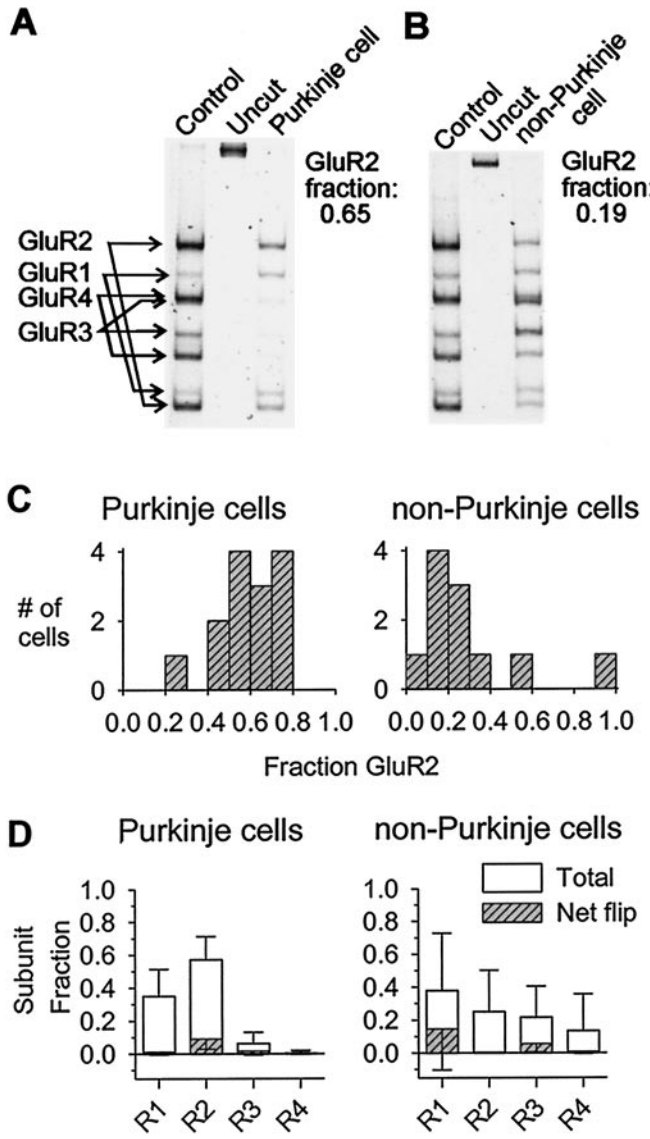

Figure 5. Subunit expression patterns in individual cerebellar neurons. Fractional AMPA subunit expression is shown in a cerebellar Purkinje neuron with high GluR2 expression (*A*) and a non-Purkinje neuron with low GluR2 expression (*B*). *C*, Distributions of the fractional GluR2 expression in all cerebellar neurons characterized as Purkinje cells (*left*) or other cerebellar cells (*right*). *D*, Summary of average ± SD subunit expression and net *flip* splice variant expression of each subunit in Purkinje cells ($n = 12$) and non-Purkinje cells ($n = 10$) in which molecular characterization was successful. Second-round PCR was often unsuccessful for subunits present in very low levels. Thus splice variant quantitation is based on fewer cells, excluding those with lowest amounts of the given subunit, and may tend to overestimate average absolute levels of a given splice variant.

Evidence has suggested that GluR2 subunits consistently contain arginine residues at the Q/R site, which controls AMPA receptor Ca^{2+} permeability, indicating that GluR2 pre-mRNA is thoroughly edited at that site in most neurons (Sommer et al., 1991; Seeburg et al., 1998). However, because incomplete editing of GluR2 in cerebellar neurons might produce a deviation from the Ca^{2+} permeability predicted on the basis of their relative expression of GluR2, the editing of the GluR2 sequences was examined in a sample of the cerebellar neurons. Using an assay based on the specific restriction digestion by the enzyme *Tse*I of

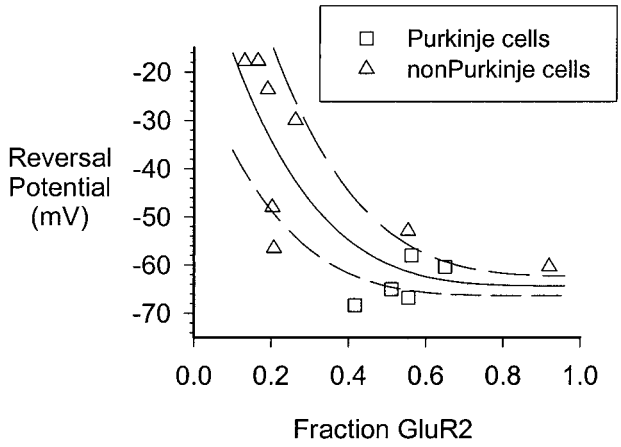

Figure 6. Molecular basis for Ca^{2+} permeability of AMPA receptors. Overall correlation of the relative Ca^{2+} permeability, as indicated by the reversal potential in 10 mM Ca^{2+}, versus the GluR2 subunit expression, is expressed as a fraction of total AMPA subunit mRNA expression. The data were fit by a modeled relationship based on stochastic assembly of subunits into tetrameric receptors (*solid line*; see Results), with confidence limits ± 1 SD (*dashed lines*) generated from estimated experimental errors.

the unedited version of the GluR2 sequence (see Materials and Methods), no evidence of incomplete editing of GluR2 was found in four Purkinje neurons and one non-Purkinje neuron (data not shown).

Relationship of Ca^{2+} permeability of expressed AMPA receptors to subunit expression patterns

In 13 cells, determinations of the *I–V* relationships were combined with successful PCR analysis, allowing comparison of the Ca^{2+} permeability to the subunit expression pattern on a cell-by-cell basis. The Ca^{2+} permeability, represented as the reversal potential in 10 mM Ca^{2+}, showed a strong negative dependence on the fractional GluR2 content in individual neurons ($r = -0.73$; $p < 0.005$, Spearman rank order correlation; Fig. 6). A similar relationship has previously been reported between relative divalent cation permeability and fractional GluR2 mRNA expression in recombinant receptors expressed in oocytes (Washburn et al., 1997) and for values averaged over cells of various types (Geiger et al., 1995), but it has not been demonstrated at the level of individual neurons.

To generate a testable model of the determination of Ca^{2+} permeability by subunit expression, some working assumptions regarding the assembly of subunits into receptors and the relationship of receptor Ca^{2+} permeability to subunit composition are required. First, the simplest model would postulate that the subunit protein levels are proportional to message levels, without assuming any post-transcriptional regulation. Next, the best present evidence suggests that each AMPA receptor contains four subunits (Rosenmund et al., 1998). Furthermore, in recombinant expression systems the evidence supports indiscriminant coassembly of different subunits based on genetic expression levels (Burnashev et al., 1992), leading to the assumption that four subunit proteins assemble in a stochastic manner; that is, each of four subunits is taken independently from the pool of AMPA subunits with a probability equal to the relative expression level. The third assumption, well supported by published data for recombinant receptors (Burnashev et al., 1992), is that GluR2 is dominant in conferring a uniformly low relative Ca^{2+} permeabil-

ity, without regard to the number of GluR2 subunits contained in the receptor. Finally, using whole-cell currents as an assay of receptor function requires assuming that receptors are inserted into surface membranes proportionately to their assembly. Taking these assumptions and representing the relative fractional expression of GluR2 as f (as message or protein), the fraction of AMPA receptors not containing any GluR2 among the four subunits is $(1 - f)^4$, and the fraction containing at least one GluR2 subunit is then $[1 - (1 - f)^4]$. Then if the reversal potential of GluR2-containing (type I) receptors is designated V_I, and that of the GluR2-lacking (type II) receptors is V_{II}, and using a linear average of the reversal potentials of individual channels to estimate the overall reversal potential (see Appendix), the predicted overall reversal potential will be:

$$V = [1 - (1 - f)^4] \cdot V_I + (1 - f)^4 \cdot V_{II}.$$

Fitting this equation to the available data by nonlinear regression gave $V_I = -64.7$ mV and $V_{II} = 9.7$ mV and the curve depicted in Figure 6 ($r = 0.83$; $p < 0.001$). This significant correlation indicates that most of the variation in the reversal potential can be explained by the differences in GluR2 mRNA levels, without postulating post-transcriptional regulation of AMPA receptor Ca^{2+} permeability. Nevertheless, some substantial deviations of the reversal potential from that predicted by this relationship occurred in individual cells.

Testing whether the deviations of the data from the predictions of the model are significant requires estimation of the experimental ("random") errors of measurements of fractional GluR2 and of the reversal potential. The SD of quantitation of fractional GluR2 content in control mixtures of cRNA (Fig. 3) averaged 0.05. However, experimental errors of fractional GluR2 measurement in single cells may exceed those in the control data, particularly if stochastic effects become large at low copy numbers of individual subunits (Sucher and Deitcher, 1995). An upper limit comes from the single-cell PCR data in Purkinje cells. If the true fractional GluR2 expression in Purkinje cells were perfectly uniform (more likely it is not), all of the variance of this measurement (mean ± SD, 0.57 ± 0.14) would come from the experimental assay. Thus the true experimental error in GluR2 measurements in single Purkinje neurons may be as low as 0.05 and is apparently not greater than ~0.14; a conservative estimate is 0.10. The experimental error of the determination of the reversal potential appears to be quite small, based on repeated determinations in the same cell, which usually differed by ≤2 mV, and on the small scatter of this value in the relatively uniform population of Purkinje cells (SD, 4 mV). An estimate of 2 mV is taken for this experimental error. Using these values to generate confidence limits on the curve relating fractional GluR2 expression to reversal potential, most of the data fell within 1 SD of the predicted relationship (Fig. 6). Thus a simple model of stochastic subunit assembly based on message levels appears to account for most of the variability in Ca^{2+} permeability among cerebellar neurons.

Fluorimetric studies of divalent cation entry via AMPA receptors

Of note, even at the highest values for fractional GluR2 expression, reversal potentials predicting a nonzero relative permeability to Ca^{2+} were measured, and small rightward shifts of the reversal potential with increased external Ca^{2+} were seen. This is consistent with studies of recombinant homomeric edited GluR2 receptors, which conducted measurable, although very small, inward Ca^{2+} currents (Burnashev et al., 1992). The Purkinje cells provide a set of morphologically identifiable cells with a predictable large GluR2 expression to answer whether native AMPA receptors in neurons expressing high GluR2 conduct physiologically significant amounts of Ca^{2+}. We examined Ca^{2+} entry in cerebellar cells by fluorimetric Ca^{2+} imaging experiments, with immunocytochemical identification of Purkinje cells after imaging experiments (Fig. 7). Kainate was applied in the absence of extracellular Na^+ to prevent Na^+-dependent depolarization and activation of voltage-gated Ca^{2+} channels. AMPA receptor activation by kainate readily induced modest increases in $[Ca^{2+}]_i$ in cytochemically identified (calbindin-positive) Purkinje neurons ($n = 16$), although the largest $[Ca^{2+}]_i$ increases occurred among the other cerebellar neurons ($n = 10$). In separate experiments (data not shown), Na^+-independent kainate-evoked $[Ca^{2+}]_i$ increases in Purkinje cells were not prevented by 30 μM La^{3+} ($n = 10$), which blocks voltage-gated Ca^{2+} channels but not Ca^{2+}-permeable AMPA receptors (Kyrozis et al., 1995). Thus, Ca^{2+} entry via AMPA receptors was sufficient to produce measurable elevations in $[Ca^{2+}]_i$ in Purkinje cells, despite their high expression of GluR2 and low overall relative Ca^{2+} permeability.

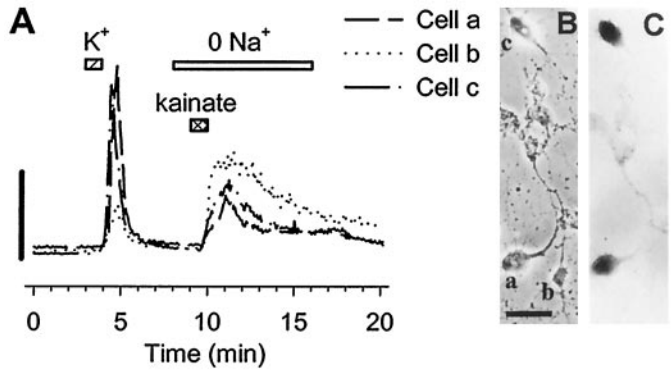

Figure 7. Kainate-induced $[Ca^{2+}]_i$ increases in Purkinje neuron. *A*, Digital fluorimetric recordings of changes in somatic $[Ca^{2+}]_i$ in representative cerebellar neurons during 1 min depolarization with 50 mM K^+ and during 1 min application of 300 μM kainate in Na^+-free solution. After imaging experiments, neurons were fixed, immunostained for calbindin D-28k (calbindin), and matched with digital images to link each $[Ca^{2+}]_i$ trace with immunostaining properties of the corresponding cell (*B*, phase-contrast image; *C*, bright-field image; neurons of 19 d *in vitro*; scale bar, 35 μm). Both calbindin-positive cells (*a*, *c*) and calbindin–negative cells (*b*) showed kainate-induced $[Ca^{2+}]_i$ increases.

DISCUSSION

Ca^{2+} entry via AMPA receptors in cerebellar Purkinje cells

Purkinje cells receive a very rich glutamatergic innervation from parallel fibers of cerebellar granule cells. AMPA receptors mediate responses at these synapses. Given their abundance of synaptically activated AMPA receptors, the strong expression of GluR2 in Purkinje cells may serve to reduce their potential for injurious Ca^{2+} overload. Although these cells express high levels of edited GluR2 and AMPA receptors with a low overall relative Ca^{2+} permeability, the present experiments show that nevertheless AMPA receptors in Purkinje cells conduct measurable Ca^{2+} currents and can account for substantial elevations in $[Ca^{2+}]_i$ under prolonged stimulation by kainate. The relationship between reversal potential and GluR2 expression demonstrates that even in the limit as fractional GluR2 approaches 1, the reversal

potentials of expressed AMPA receptors approach a value consistent with a residual small Ca^{2+} permeability. Indeed, previous reports indicated that even homomeric GluR2 AMPA receptors had reversal potentials suggesting a small Ca^{2+} permeability, similar to those of heteromeric receptors from combined expression of GluR2 and GluR4 (Burnashev et al., 1992). Studies of AMPA receptors in glial cell precursors, using the selective antagonists Joro spider toxin and argiotoxin, also indicated that GluR2-containing receptors contributed substantial portions of the measured Ca^{2+} influx (Meucci et al., 1996). In sum, evidence suggests that the Ca^{2+} fluxes detected in GluR2-expressing neurons are carried not only by a few highly permeable receptors lacking GluR2 subunits but also by the larger number of receptors containing edited GluR2 subunits, which retain a low Ca^{2+} permeability. The proportional contribution of each type of receptor to the total Ca^{2+} influx in each cell appears to depend strongly on the fractional GluR2 expression.

As previously reported (Geiger et al., 1995; Washburn et al., 1997), the relative divalent cation permeability of AMPA receptors is a steep negative function of fractional GluR2 expression in the lower range, giving rise to intermediate values of $P_{Ca^{2+}}/P_{Cs^+}$ in cells expressing small amounts of GluR2 (Jonas et al., 1994; Lerma et al., 1994; Goldstein et al., 1995). In Purkinje cells, previous patch-clamp studies of Ca^{2+} permeability of AMPA receptors produced estimates of 0.17 for $P_{Ca^{2+}}/P_{Na^+}$ in cultured neurons (Linden et al., 1993) and of 0.19 for $P_{Ca^{2+}}/P_{Cs^+}$ in a slice preparation (Tempia et al., 1996), compared with the values of $P_{Ca^{2+}}/P_{Cs^+}$ found in Purkinje cells in the present studies of 0.22 in the NMG-based solution and 0.10 in the sucrose-based solution. In other neurons that express GluR2 strongly, previous estimates of divalent permeability of AMPA receptors have generally suggested values for $P_{Ca^{2+}}/P_{Cs^+}$ of ~0.1 or less (Jonas et al., 1994; Lerma et al., 1994; Geiger et al., 1995). These different values for $P_{Ca^{2+}}/P_{Cs^+}$ measured under various ionic conditions likely arise in part from differing assumptions regarding ionic activities and permeabilities, but they may also arise from failure of some of the assumptions of the GHK theory. In particular, the postulate of ionic independence may not describe well the interaction in the ion pore of a large cation such as NMG, with slight permeability (Burnashev et al., 1996), and other cations. Whatever assumptions are made, it is clear that the relative permeability to Ca^{2+} of AMPA receptors in Purkinje cells is low.

Previous $[Ca^{2+}]_i$ fluorimetry experiments in Purkinje cells in cerebellar slices found little $[Ca^{2+}]_i$ change attributable to direct Ca^{2+} entry via AMPA receptors and estimated that only 0.6% of the total inward current through AMPA receptors was carried by Ca^{2+} (Tempia et al., 1996). The reasons that the present experiments measured larger $[Ca^{2+}]_i$ increases in Purkinje cells stimulated by kainate may relate to technical differences, such as different levels of introduced chelators or of native $[Ca^{2+}]_i$ buffering systems in Purkinje cells in two preparations. The present studies are in agreement with the results of Tempia et al. (1996) in that the Purkinje cells consistently express GluR2 and have a low overall relative Ca^{2+} permeability. Whether the small residual amounts of Ca^{2+} entry have physiological significance may depend on to what degree AMPA receptors, like NMDA receptors, are directly linked to Ca^{2+}-dependent effector molecules, allowing localized domains of $[Ca^{2+}]_i$ increases to induce specific effects. Our previous results have shown that, at least in cultured Purkinje cells, such Ca^{2+} fluxes can have pathophysiological significance (Brorson et al., 1994).

The determination of AMPA receptor Ca^{2+} permeability

The ability of the simple model presented here for determination of reversal potential by fractional GluR2 expression to account for most of the variability in Ca^{2+} permeability among neurons suggests that receptor expression may mainly be determined by regulation of subunit transcription, with stochastic association of subunit proteins, present at levels proportional to mRNA levels. The elements of this model have been proposed previously, including calculation of contributions of two receptor types by a combinatorial approach (Geiger et al., 1995; Washburn et al., 1997), but its application has not previously been demonstrated in native AMPA receptor populations in individual neurons.

Some reports have described selective localization of subsets of expressed receptors to regions of certain neurons (Craig et al., 1993; Lerma et al., 1994; Miyashiro et al., 1994; Rubio and Wenthold, 1997). The present data only assess overall AMPA receptor expression, measured as whole-cell current responses, and do not rule out regional differences in mRNA transport or in insertion of subunits into surface membranes. In fact, recent evidence has suggested important localization of GluR2-lacking AMPA receptors to a subset of synapses on hippocampal interneurons (Tóth and McBain, 1998). It may be that detailed subcellular studies of receptor expression will provide increasing examples of synaptic specialization for certain AMPA receptor properties. Furthermore, these data cannot rule out more complex schemes, such as one in which GluR2 subunits are selectively incorporated into AMPA receptors in a given cell type, such as Purkinje cells. In such a case, feedback regulation of subunit transcription might also allow message levels to match those predicting the Ca^{2+} permeability, on a secondary basis. Also, the precision of the determination of fractional subunit levels is not sufficient to rule out small contributions to AMPA receptor expression by post-transcriptional regulation of subunit protein synthesis. Nevertheless, in the absence of data requiring postulation of additional levels of regulation, the simplest model appears to be sufficient: that at the whole-cell level, functional receptor expression is consistent with determination of AMPA receptor composition primarily at the level of transcription.

The determination of AMPA receptor Ca^{2+} permeation properties is an issue of possible therapeutic importance. A downward shift in GluR2 expression in CA1 hippocampal pyramidal neurons after global ischemia has been proposed as a reason for the selective delayed death of these neurons attributable to Ca^{2+} entry via AMPA receptors (Pellegrini-Giampietro et al., 1992). In another example, spinal motor neurons may be vulnerable to abnormal glutamate exposures because of Ca^{2+} permeation via AMPA receptors (Carriedo et al., 1996; Vandenberghe et al., 1998), despite reports of detectable GluR2 in these cells (Tölle et al, 1993). In fact, most neurons express GluR2. Selective pharmacological blockade of Ca^{2+} entry as a therapeutic scheme in AMPA receptor-mediated neurotoxicity will depend on clarifying the relative importance of Ca^{2+} influx by rare GluR2-lacking receptors of high Ca^{2+} permeability versus influx by numerous GluR2-containing receptors of low relative Ca^{2+} permeability.

APPENDIX: MODELING DETERMINATION OF WHOLE-CELL REVERSAL POTENTIAL BY GluR2 EXPRESSION

If type I channels, containing GluR2, and type II channels, lacking GluR2, are approximated near their reversal potentials V_I and V_{II} by linear I–V relationships with slope conductances S_I and S_{II}, then the I–V relationships for the channels are described by I_I

$= S_I \cdot (V - V_I)$ and $I_{II} = S_{II} \cdot (V - V_{II})$. If the numbers of each type of channel are N_I and N_{II}, then the total current I_T will be:

$$I_T = N_I \cdot I_I + N_{II} \cdot I_{II} = N_I \cdot S_I \cdot (V - V_I) + N_{II} \cdot S_{II} \cdot (V - V_{II}).$$

The reversal potential of the total current will be V_0 such that $I_T(V_0) = 0$. Solving for V_0 gives:

$$V_0 = [N_I \cdot S_I \cdot V_I + N_{II} \cdot S_{II} \cdot V_{II}]/[N_I \cdot S_I + N_{II} \cdot S_{II}]$$
$$= [n_I \cdot V_I + n_{II} \cdot s \cdot V_{II}]/[n_I + n_{II} \cdot s], \quad (1)$$

where $n_I = N_I/(N_I + N_{II})$ and $n_{II} = N_{II}/(N_I + N_{II})$ are the fractional representations of each channel type, and $s = S_{II}/S_I$ is the relative slope conductance. For $s = 1$, using $n_I + n_{II} = 1$, the equation simplifies to:

$$V_0 = n_I \cdot V_I + n_{II} \cdot V_{II}. \quad (2)$$

Based on the several assumptions described in Results, with the number of subunits per receptor as n and the relative fractional expression of GluR2 as f, the fraction of AMPA receptors lacking GluR2 among the four subunits is $n_{II} = (1\text{-}f)^n$, and the fraction containing at least one GluR2 subunit is then $n_I = [1 - (1 - f)^n]$. Then, for the case of $s = 1$, the predicted overall reversal potential will be:

$$V_0 = [1 - (1 - f)^n] \cdot V_I + (1 - f)^n \cdot V_{II}. \quad (3)$$

If the average slope conductances are different ($s \neq 1$), a substantially more complicated expression results:

$$V_0 = \{[1 - (1 - f)^n] \cdot V_I + (1 - f)^n \cdot s \cdot V_{II}\}/$$
$$\{[1 - (1 - f)^n] + (1 - f)^n \cdot s\}. \quad (4)$$

Present evidence suggests tetrameric AMPA receptors ($n = 4$) (Rosenmund et al., 1998), although previously they have also been modeled as pentamers. Swanson et al. (1997) found that recombinant AMPA receptor single channels lacking GluR2 open to higher conductance states than GluR2 and GluR4 heteromers, and that GluR2 homomeric channels have very low conductance. GluR2 homomers would be present in significant numbers only at the highest values of f and would decrease the total current through type I channels without significantly affecting overall permeability if GluR2 is truly dominant in determining Ca^{2+} permeability. Thus, their effect on the relationship between reversal potential and f can be neglected. S_I and S_{II}, needed for the present model, represent the time-averaged conductance over all open states for each channel type, and these values are not readily available from the literature. If the average conductance difference between type I and type II channels is small ($s \sim 1$), Equation 3 can be used to fit the observed data, with two free parameters, V_I and V_{II}. If the conductance difference is significant, then Equation 4, with three parameters, s, V_I, and V_{II}, will be required to fit the data well.

Results and Figure 5 describe nonlinear regression fitting of Equation 3 to the data using $n = 4$. The fit of the data using Equation 4 was insensitive to the alternative choices $n = 4$ or 5 with $s = 1$ ($r = 0.83$ for $n = 4$, $s = 1$; $r = 0.84$ for $n = 5$, $s = 1$), but the correlation coefficient fell with increasing values of $s = 2$, 5, or 10 (to $r = 0.77$ for $n = 5$, $s = 10$; $r = 0.73$ for $n = 4$, $s = 10$). Thus important differences in the time-averaged conductance of type I and type II channels were not indicated by this analysis.

REFERENCES

Audinat E, Knopfel T, Gahwiler BH (1990) Responses to excitatory amino acids of Purkinje cells and neurones of the deep nuclei in cerebellar slice cultures. J Physiol (Lond) 430:297–313.

Bochet P, Audinat E, Lambolez B, Crépel F, Rossier J, Iino M, Tsuzuki K, Ozawa S (1994) Subunit composition at the single-cell level explains functional properties of a glutamate-gated channel. Neuron 12:383–388.

Brorson JR, Bleakman D, Chard PS, Miller RJ (1992) Calcium directly permeates kainate/α-amino-3-hydroxy-5-methyl-4-isoxazolepropionic acid receptors in cultured cerebellar Purkinje neurons. Mol Pharmacol 41:603–608.

Brorson JR, Manzolillo PA, Miller RJ (1994) Ca^{2+} entry via AMPA/KA receptors and excitotoxicity in cultured cerebellar Purkinje cells. J Neurosci 14:187–197.

Brorson JR, Manzolillo PA, Gibbons SJ, Miller RJ (1995) AMPA receptor desensitization predicts the selective vulnerability of cerebellar Purkinje cells to excitotoxicity. J Neurosci 15:4515–4524.

Burnashev N, Monyer H, Seeburg PH, Sakmann B (1992) Divalent ion permeability of AMPA receptor channels is dominated by the edited form of a single subunit. Neuron 8:189–198.

Burnashev N, Villarroel A, Sakmann B (1996) Dimensions and ion selectivity of recombinant AMPA and kainate receptor channels and their dependence on Q/R site residues. J Physiol (Lond) 496:165–173.

Carriedo SG, Yin HZ, Weiss JH (1996) Motor neurons are selectively vulnerable to AMPA/kainate receptor-mediated injury *in vitro*. J Neurosci 16:4069–4079.

Craig AM, Blackstone CD, Huganir RL, Banker G (1993) The distribution of glutamate receptors in cultured rat hippocampal neurons: postsynaptic clustering of AMPA-selective subunits. Neuron 10:1055–1068.

Dean JA (1992) Lange's handbook of chemistry, Ed 14. New York: McGaw-Hill.

Geiger JRP, Melcher T, Koh D-S, Sakmann B, Seeburg PH, Jonas P, Monyer H (1995) Relative abundance of subunit mRNAs determines gating and Ca^{2+} permeability of AMPA receptors in principal neurons and interneurons in rat CNS. Neuron 15:193–204.

Goldstein PA, Lee CJ, MacDermott AB (1995) Variable distributions of Ca^{2+}-permeable and Ca^{2+}-impermeable AMPA receptors on embryonic rat dorsal horn neurons. J Neurophysiol 73:2522–2534.

Hodgkin AL, Katz B (1949) The effect of sodium ions on the electrical activity of the giant axon of the squid. J Physiol (Lond) 108:37–77.

Hollmann M, Hartley M, Heinemann S (1991) Ca^{2+} permeability of KA-AMPA-gated glutamate receptor channels depends on subunit composition. Science 252:851–853.

Iino M, Ozawa S, Tsuzuki K (1990) Permeation of calcium through excitatory amino acid receptor channels in cultured rat hippocampal neurones. J Physiol (Lond) 424:151–165.

Isa T, Itazawa S-I, Iino M, Tsuzuki K, Ozawa S (1996) Distribution of neurones expressing inwardly rectifying and Ca^{2+}-permeable AMPA receptors in rat hippocampal slices. J Physiol (Lond) 491:719–733.

Jan LY, Jan YN (1976) L-glutamate as an excitatory transmitter at the *drosophila* larval neuromuscular junction. J Physiol (Lond) 262:215–236.

Jonas P, Racca C, Sakmann B, Seeburg PH, Monyer H (1994) Differences in Ca^{2+} permeability of AMPA-type glutamate receptor channels in neocortical neurons caused by differential GluR-B subunit expression. Neuron 12:1281–1289.

Kyrozis A, Goldstein PA, Heath MJ, MacDermott AB (1995) Calcium entry through a subpopulation of AMPA receptors desensitized neighbouring NMDA receptors in rat dorsal horn neurons. J Physiol (Lond) 485:373–381.

Lambolez B, Audinat E, Bochet P, Crépel F, Rossier J (1992) AMPA receptor subunits expressed by single Purkinje cells. Neuron 9:247–258.

Lerma J, Morales M, Ibarz JM, Somohano F (1994) Rectification properties and Ca^{2+} permeability of glutamate receptor channels in hippocampal cells. Eur J Neurosci 6:1080–1088.

Linden DJ, Smeyne M, Connor JA (1993) Induction of cerebellar long-term depression in culture requires postsynaptic action of sodium ions. Neuron 11:1093–1100.

Mayer ML, Westbrook GL (1987) Permeation and block of *N*-methyl-D-aspartic acid receptor channels by divalent cations in mouse cultured central neurons. J Physiol (Lond) 394:501–527.

Meucci O, Fatatis A, Holzwarth JA, Miller RJ (1996) Developmental regulation of the toxin sensitivity of Ca^{2+}-permeable AMPA receptors in cortical glia. J Neurosci 16:519–530.

Miyashiro K, Dichter M, Eberwine J (1994) On the nature and differential distribution of mRNAs in hippocampal neurites: Implications for neuronal functioning. Proc Natl Acad Sci USA 91:10800–10804.

Otis TS, Raman IM, Trussell LO (1995) AMPA receptors with high Ca^{2+} permeability mediate synaptic transmission in the avian auditory pathway. J Physiol (Lond) 482:309–315.

Pellegrini-Giampietro DE, Zukin RS, Bennett MVL, Cho S, Pulsinelli WA (1992) Switch in glutamate receptor subunit gene expression in CA1 subfield of hippocampus following global ischemia in rats. Proc Natl Acad Sci USA 89:10499–10503.

Rosenmund C, Stern-Bach Y, Stevens CF (1998) The tetrameric structure of a glutamate receptor channel. Science 280:1596–1599.

Rubio ME, Wenthold RJ (1997) Glutamate receptors are selectively targeted to postsynaptic sites in neurons. Neuron 18:939–950.

Seeburg PH, Higuchi M, Sprengel R (1998) RNA editing of brain glutamate receptor channels: mechanism and physiology. Brain Res Rev 26:217–229.

Sommer B, Kohler M, Sprengel R, Seeburg PH (1991) RNA editing in brain controls a determinant of ion flow in glutamate-gated channels. Cell 67:11–19.

Sucher NJ, Deitcher DL (1995) PCR and patch-clamp analysis of single neurons. Neuron 14:1095–1100.

Swanson GT, Kamboj SK, Cull-Candy SG (1997) Single-channel properties of recombinant AMPA receptors depend on RNA editing, splice variation, and subunit composition. J Neurosci 17:58–69.

Tempia F, Kano M, Schneggenburger R, Schirra C, Garaschuk O, Plant T, Konnerth A (1996) Fractional calcium current through neuronal AMPA-receptor channels with a low calcium permeability. J Neurosci 15:456–466.

Tölle TR, Berthele A, Zieglgänsberger W, Seeburg PH, Wisden W (1993) The differential expression of 16 NMDA and non-NMDA receptor subunits in the rat spinal cord and in periaqueductal gray. J Neurosci 13:5009–5028.

Tóth K, McBain CJ (1998) Afferent-specific innervation of two distinct AMPA receptor subtypes on single hippocampal interneurons. Nat Neurosci 1:572–578.

Turetsky DM, Canzoniero LMT, Sensi SL, Weiss JH, Goldberg MP, Choi DW (1994) Cortical neurons exhibiting kainate-activated Co^{2+} uptake are selectively vulnerable to AMPA/kainate receptor-mediated toxicity. Neurobiol Dis 1:101–110.

Vandenberghe W, Van Den Bosch L, Robberecht W (1998) Glial cells potentiate kainate-induced neuronal death in a motoneuron-enriched spinal coculture system. Brain Res 807:1–10.

Washburn MS, Numberger M, Zhang S, Dingledine R (1997) Differential dependence on GluR2 expression of three characteristic features of AMPA receptors. J Neurosci 17:9393–9406.

Zhang D, Sucher NJ, Lipton SA (1995) Co-expression of AMPA/kainate receptor-operated channels with high and low Ca^{2+} permeability in single rat retinal ganglion cells. Neuroscience 67:177–188.